

can be represented by storing one occurrence of the pattern and the translation vectors required to produce all other occurrences of  $P$  [11].

#### 4. THE SIATEC-C ALGORITHM

The SIATEC-C algorithm computes TECs of patterns in a point-set  $D$ , such that, the IOI between adjacent points in a pattern is at most a given threshold  $\delta$ . SIATEC-C also avoids producing small patterns when the points covered by the pattern are already covered by a larger discovered pattern. SIATEC-C thus avoids producing patterns with isolated members while reducing the running time and memory footprint. This approach aims at similar results as compactness trawling in [19]. Cutting patterns at large IOI gaps has also been suggested in [29].

The outline of SIATEC-C is described in algorithm 1. The pseudocode aims at a concise presentation of the algorithm. A more thorough pseudocode description and a reference implementation of the algorithm that covers all details is also made available<sup>1</sup>. The algorithm takes as its inputs a point-set  $D$  and the IOI threshold  $\delta$ . The first components of the points are assumed to represent onset times of note events. The algorithm outputs the discovered patterns and all of their occurrences represented as TECs.

The algorithm begins by sorting the input point-set in ascending lexicographical order to produce the point-set  $D_s$ . The variables  $T$  and  $W$  are used for tracking a sliding window for each point in  $D_s$  in the onset dimension. The sliding windows are used in computing MTPs in order to restrict the number of MTPs that need to be kept in memory simultaneously. The array  $T$  keeps track of the index from where to continue computation on each iteration, and the array  $W$  keeps track of the upper bounds of the windows. The indexing in the pseudocode starts at 1 and array access is denoted by brackets. For  $T$  the value at index  $i$  stores the index in  $D_s$  for where the next sliding window starts. The value at index  $i$  of  $W$  stores the upper bound of the sliding window for the  $i$ th point of  $D_s$ . The indices in  $T$  are initialized to the range from 1 to  $n$  (line 4) and on line 5 the upper bounds are initialized for each point  $p \in D_s$  to be  $p.x + \delta$ . The values in the array  $C$  keep track of the size of the largest pattern occurrence that covers the corresponding point in  $D_s$ .

The *difference index* structure  $I$  is computed by the COMPUTEDIFFINDEX function. Difference vectors between all pairs of points,  $p_i$  and  $p_j$ , for which the IOI between the points does not exceed the threshold  $\delta$ , are computed. The differences along with the index-pairs  $\langle i, j \rangle$  are stored in the intermediate array  $I'$ . The array is sorted in ascending lexicographical order by the difference vectors and indices. The sorted array is partitioned by the difference vectors, so that an array of entries of the form  $\langle v, [\langle s_1, t_1 \rangle, \dots, \langle s_i, t_i \rangle] \rangle$  is created. Each entry contains a difference vector  $v$  and the corresponding *source* and *target* indices. The source indices  $s_i$  are the indices of points in  $D_s$  that can be translated by  $v$  within  $D_s$ , and the corre-

---

#### Algorithm 1 SIATEC-C Algorithm

---

```

1: function SIATEC-C( $D, \delta$ )
2:    $D_s \leftarrow \text{SORT}_{Lex}(D)$ 
3:    $n \leftarrow |D_s|$ 
4:    $T \leftarrow [1, 2, \dots, n]$ 
5:    $W \leftarrow \text{INITWINDOWBOUNDS}(D_s, \delta)$ 
6:    $C \leftarrow [0, 0, \dots, 0]$  of  $n$  zeros
7:    $I \leftarrow \text{COMPUTEDIFFINDEX}(D_s, \delta)$ 
8:   while  $T[1] \leq n$  do
9:      $M \leftarrow \text{COMPUTEMTPS}(D_s, T, W)$ 
10:     $M' \leftarrow \text{CUTANDSORT}(M, \delta)$ 
11:    for  $P \in M'$  do
12:      if  $\text{IMPROVESCOVER}(P, C)$  then
13:         $\text{FINDTRANSLATORS}(P, I, D_s, C)$ 
14:       $\text{OUTPUTTEC}$ 

```

---

sponding target indices are of the points that are produced by translating the point at the source index by  $v$ . The index structure  $I$  is sorted in ascending order of difference vectors and all source and target indices for an entry are also in ascending order.

In the main loop of the SIATEC-C algorithm (lines 8–14 of 1), MTPs are computed for translation vectors within the sliding windows by the COMPUTEMTPS function. The MTPs are computed by first computing all translations between pairs of points where the target point is within the sliding window of the source point. The indices of the source points are stored in pairs with the translations. The array thus produced is sorted in ascending lexicographical order and partitioned by the translation vectors. The function is otherwise equal to the SIA algorithm [11], except that the difference vectors are limited by the sliding windows defined by the arrays  $T$  and  $W$ , and the indices of the MTP and its translated occurrence are also stored. The sliding windows are used to avoid keeping all  $O(n^2)$  differences in memory at the same time. On each iteration the indices in  $T$  are updated to the point just outside the current window and then the sliding window upper bounds in  $W$  are incremented by  $\delta$ .

The produced MTPs can have gaps in them that exceed the threshold  $\delta$ . Thus the MTPs are cut on line 10 to produce the set of patterns  $M'$ , where the IOI between no adjacent patterns points exceeds  $\delta$ . The patterns are also sorted in descending order of size to ensure that larger patterns are handled first. The function IMPROVESCOVER checks if the pattern, or its translated version, is larger than any of the patterns that cover the same points. A pattern is considered to improve the cover only if it improves the cover value of at least one point. This step reduces the number of small and duplicate patterns that would be otherwise output by the algorithm. Small patterns may be output by the algorithm even if a larger pattern covering the same points is discovered. This occurs in the case that the small pattern is found on an earlier iteration of the main loop (lines 8–14).

<sup>1</sup> <https://github.com/otsob/siatec-c-code>

#### 4.1 Finding translators

Finding the translators of a pattern  $P$  is achieved by traversing the index-pairs stored in  $I$  using the vectors of the vectorized representation  $VEC(P)$ . This is equivalent to finding translationally equivalent prefixes of  $P$  and extending the prefixes until they are equal in length to  $P$ .

---

**Algorithm 2** SIATEC-C: Find translators and update cover
 

---

```

1: function FINDTRANSLATORS( $P, I, D_s, C$ )
2:    $V \leftarrow VEC(P)$ 
3:    $v \leftarrow V[1]$ 
4:    $A \leftarrow \{ t \mid \langle s, t \rangle \in \text{FINDINDICES}(v, I) \}$ 
5:   for  $i \in [2, \dots, |V|]$  do
6:      $v \leftarrow V[i]$ 
7:      $A' \leftarrow \text{FINDINDICES}(v, I)$ 
8:      $A \leftarrow \{ t \mid \langle s, t \rangle \in A' \wedge s \in A \}$ 
9:    $l \leftarrow P[|P|]$ 
10:   $\tau \leftarrow \{ D_s[i] - l \mid i \in A \}$ 
11:   $C \leftarrow \text{UPDATECOVER}(P, A, C, I)$ 
12:  return  $\tau$ 
    
```

---

Figure 1 illustrates the process of finding the translators of a pattern  $P$ ,  $VEC(P) = [v, u]$  with a very minimal point-set example. The crosses and points form two three-point patterns that are translationally equivalent. First binary search is used to find the index pairs for  $v$  from  $I$ , returning the index pairs  $[(1, 2), \langle 4, 5)]$ . The second elements of these pairs are the indices of points that can be translated with  $u$  to continue translationally equivalent prefixes of  $P$ . On the next iteration the index-pairs associated with  $u$  are retrieved producing the index-pairs  $[(2, 3), \langle 5, 6)]$ . The target indices 2 and 5 of the vector  $v$  are matched with the source indices of  $u$  to find that the translationally equivalent prefixes can be extended with the points at indices 3 and 6 to find the last points of translationally equivalent occurrences of  $P$ . The translators can be computed simply as the difference between the last points of the found occurrences and the last point of  $P$ .

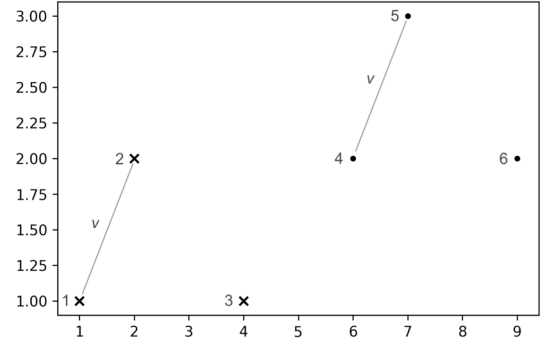
#### 4.2 Time and space complexity

The following theorems present the worst case time and space complexity of SIATEC-C.

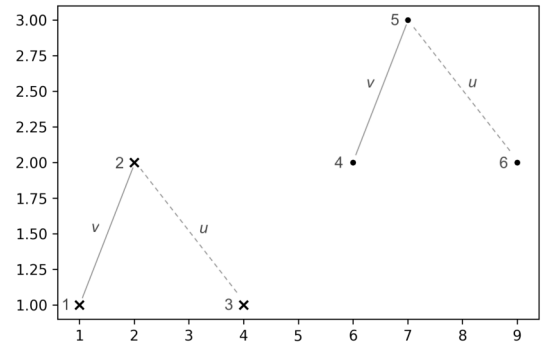
**Theorem 4.1.** *Let  $D$  be a 2-dimensional point-set with  $n$  points. Let  $m$  be the largest number of points in any span of length  $\delta$  in the onset dimension and let  $h$  be the number of points in the largest MTP in  $D$ . Then the worst case time complexity of SIATEC-C is  $O(hn^2 \log nm)$ .*

*Proof.* Computing the difference index  $I$  requires computing  $O(nm)$  difference vectors, sorting them, and partitioning. Thus COMPUTEDIFFINDEX runs in  $O(nm \log nm)$  time.

The number of iterations the main loop on lines 8–14 of algorithm 1 executes is approximately  $\frac{n}{\delta} = O(n)$ . Computing the MTPs requires also computing  $O(nm)$  difference vectors, sorting and partitioning them into MTPs, and then sorting the MTPs by size, thus running in



(a) Step 1: Prefix of length 2



(b) Step 2: Prefix of length 3

**Figure 1:** FINDTRANSLATORS example

$O(nm \log nm)$  time. However, the total amount of computation required to compute MTPs in the loop performs the same number of difference vector computations and comparisons as computing all MTPs and sorting them by size, thus the total amount of work needed for MTP computation during the execution of the algorithm is  $O(n^2 \log n)$  just as in SIA [11].

For a pattern  $P$ , the size of its vectorized representation is  $|P| - 1$ . The FINDTRANSLATORS function is thus run on  $O(n^2)$  difference vectors in total. For each difference vector, the loop finds the index pairs from  $I$  in  $O(\log nm)$  time using binary search and computes the intersection of  $A$  with the source indices in  $A'$ . The number of index pairs that can be found for a difference vector  $v$  in  $I$  is equal to the size of the largest MTP in  $D$ , denoted by  $h$ . Thus computing the intersection of sorted arrays is linear in  $h$ , resulting in time complexity of  $O(h \log nm)$  for a single difference vector in  $\vec{P}$ . Overall, finding all translators for all produced patterns has a worst case time complexity of  $O(hn^2 \log nm)$ .

The overall worst case time complexity of the algorithm is thus dominated by computing the translators, resulting in a worst case time complexity of  $O(hn^2 \log nm)$ .  $\square$

**Theorem 4.2.** *Let  $D$  be a 2-dimensional point-set with  $n$  points, and let  $m$  be the largest number of points in any span of length  $\delta$  in the onset dimension. Then the worst case space complexity of SIATEC-C is  $O(nm)$ .*

*Proof.* Computing the difference index  $I$  requires storing  $O(nm)$  difference vectors and corresponding index pairs, and after partitioning the number of difference vectors and index pairs does not increase. Therefore  $I$  takes  $O(nm)$  space.

On each iteration of the main loop on lines 8–14 of algorithm 1 the MTP computation requires keeping  $O(nm)$  difference vectors in memory.

In the FINDTRANSLATORS function the number of index pairs contained in  $A$  or  $A'$  is at most the equal to the size of the largest MTP in  $D$ . Therefore the space complexity of FINDTRANSLATORS is  $O(n)$ .

The space complexity of SIATEC-C is dominated by  $I$  and the MTP computation, therefore the worst case space complexity is  $O(nm)$ .  $\square$

## 5. RESULTS

This section contains the computational performance results of the SIATEC-C algorithm and its evaluation on the JKU-PDD dataset.

### 5.1 Computational Performance

The running time and memory usage of the SIA, SIAR ( $r = 1$ ), SIATEC, and SIATEC-C algorithms was measured on two types of point-sets:  $D_{min}$  and random patterns. The point-set sizes ranged from 1000 to 10000 in increments of 1000. The  $D_{min}$  dataset was chosen as it produces the worst-case running time of SIATEC-C and can thus provide an estimate of the upper bound of running time and memory usage. Random patterns were used instead of concatenating short pieces of music together to control the sizes of MTPs in the benchmark data.

The algorithms were implemented using the Rust<sup>2</sup> programming language. The measurements were performed on a machine running Ubuntu 20.04 with an Intel i7-processor and 16GB of memory. The IOI threshold parameter  $\delta$  of SIATEC-C was set to a 50.0 for the artificial point-sets, for music point-sets  $\delta = 4$  was used throughout, corresponding to one measure in  $\frac{4}{4}$  time.

The measurements for running times are plotted in figure 2 and the maximum heap usage measurements are plotted in figure 3. Log-scale is used on the  $y$ -axis as the measurements vary greatly in the range of values. The most significant running time improvements SIATEC-C can provide compared to SIATEC can be seen in the plot for the running time on the random pattern point-sets. Even with the largest point-sets, the running time of SIATEC-C is 22.2s, while the running time of SIATEC exceeds 2500s. On random pattern point-sets SIAR is the fastest algorithm.

In the case of the  $D_{min}$  point-sets the running time of SIATEC and SIATEC-C behaves relatively similarly. With

SIAR the  $D_{min}$  produces worst-case performance leading the performance of SIAR to be comparable to that of SIA. This is explained by the worst-case time complexity of SIAR, which on a  $k$ -dimensional point-set of size  $n$  is  $O(kn^3)$  [30].

The memory usage was measured using the Heaptrack software<sup>3</sup> that only measures heap memory. With the largest random patterns point-set SIATEC-C uses only 26.08MB and with the largest  $D_{min}$  point-set 78.20MB.

On the random patterns point-sets SIAR runs with the smallest memory footprint. However, the  $D_{min}$  point-sets illustrates the quadratic space complexity of SIAR [30], with the memory footprint of SIAR exceeding that of SIATEC-C. Thus replacing SIA with SIAR in SIATEC will not guarantee a smaller memory footprint than can be obtained with SIATEC-C.

SIAR can be a very performant algorithm on many point-sets, however, its performance varies greatly depending on the size of the largest MTPs in the input point-set. In order to investigate the impact of the worst-case time and space complexities between SIATEC-C and SIAR, both algorithms were run on a point-set representation<sup>4</sup> of Beethoven’s 9th symphony ( $n = 107,355$ ). SIATEC-C ( $\delta = 4$ ) ran in approximately 28 minutes with peak heap usage of 1.97GB while SIAR ( $r = 1$ ) ran in approximately 1 hour 7 minutes with peak heap usage 5.64GB. While SIAR can be the most performant algorithm on small point-sets, due to its worst-case time and space complexity there is no guarantee that it will be the most performant on large point-sets.

### 5.2 Evaluation on JKU-PDD

The accuracy of the SIATEC-C algorithm was evaluated on the JKU-PDD data set [31]. A version of SIATEC-C without any post-processing was evaluated to investigate whether it is capable of achieving establishment precision and recall comparable to other point-set algorithms that have been shown to benefit from post-processing, e.g., compactness trawling [26, 28].

The COSIATEC and SIATECCompress compression algorithms [22] produce a compressed representation of the input point-set by selecting TECs produced by SIATEC. The algorithms COSIATEC-C and SIATECCompress are otherwise equal to COSIATEC and SIATECCompress except they use SIATEC-C instead of SIATEC for producing TECs.

Table 1 displays the mean values of the MIREX metrics over the monophonic and polyphonic corpus of JKU-PDD. Compared to SIATEC and SIAR, SIATEC-C produces fewer patterns and achieves slightly improved establishment precision and recall.

## 6. DISCUSSION AND CONCLUSION

In this paper we have presented a novel algorithm SIATEC-C for repeated pattern discovery in symbolic polyphonic

<sup>2</sup> <https://www.rust-lang.org>

<sup>3</sup> <https://github.com/KDE/heaptrack>

<sup>4</sup> Converted from <https://musescore.com/openscore/scores/5733014>.

Algorithm	Corpus	$N_{points}$	$N_{patterns}$	$N_{pt}$	$P_{rat}$	$R_{rat}$	$F1_{rat}$	$P_{3L}$	$R_{3L}$	$F1_{3L}$	$P_{occ}(c=0.75)$	$R_{occ}(c=0.75)$	$F1_{occ}(c=0.75)$	$P_{occ}(c=0.5)$	$R_{occ}(c=0.5)$	$F1_{occ}(c=0.5)$
SIATEC	monophonic	677.2	30014.8	6.2	0.128	0.679	0.208	0.072	0.613	0.125	0.681	0.569	0.617	0.459	0.561	0.503
SIATEC-C ( $\delta=4$ )	monophonic	677.2	970.0	6.2	<b>0.189</b>	<b>0.890</b>	<b>0.308</b>	<b>0.131</b>	<b>0.852</b>	<b>0.227</b>	<b>0.842</b>	<b>0.854</b>	<b>0.844</b>	<b>0.558</b>	<b>0.824</b>	<b>0.649</b>
SIAR ( $r=1$ )	monophonic	677.2	5365.0	6.2	0.148	0.679	0.236	0.091	0.505	0.149	0.685	0.422	0.509	0.496	0.391	0.424
COSIATEC	monophonic	677.2	15.2	6.2	0.136	0.234	0.169	0.085	0.199	0.117	0.165	0.165	0.165	0.256	0.192	0.219
SIATECCompress	monophonic	677.2	10.6	6.2	0.124	0.116	0.068	0.091	0.075	0.000	0.000	0.000	0.000	0.000	0.000	0.000
COSIATEC-C	monophonic	677.2	28.8	6.2	0.090	0.214	0.124	0.088	0.217	0.122	0.000	0.000	0.000	0.000	0.038	0.058
SIATEC-CCompress	monophonic	677.2	21.4	6.2	0.087	0.148	0.109	0.068	0.130	0.088	0.200	0.110	0.142	0.200	0.110	0.142
SIATEC	polyphonic	1289.0	59081.8	5.4	0.105	0.690	0.178	0.066	0.595	0.117	0.677	0.543	0.593	0.499	0.530	0.501
SIATEC-C ( $\delta=4$ )	polyphonic	1289.0	977.6	5.4	<b>0.131</b>	<b>0.775</b>	<b>0.217</b>	<b>0.097</b>	<b>0.675</b>	<b>0.164</b>	<b>0.868</b>	<b>0.708</b>	<b>0.759</b>	0.570	<b>0.645</b>	<b>0.577</b>
SIAR ( $r=1$ )	polyphonic	1289.0	12721.4	5.4	0.116	0.635	0.195	0.089	0.483	0.147	0.683	0.476	0.544	<b>0.588</b>	0.419	0.477
COSIATEC	polyphonic	1289.0	19.6	5.4	0.091	0.196	0.122	0.056	0.172	0.083	0.157	0.157	0.157	0.290	0.224	0.253
SIATECCompress	polyphonic	1289.0	15.8	5.4	0.103	0.121	0.108	0.059	0.092	0.069	0.000	0.000	0.000	0.000	0.000	0.000
COSIATEC-C	polyphonic	1289.0	41.2	5.4	0.070	0.161	0.095	0.058	0.143	0.081	0.000	0.000	0.000	0.000	0.019	0.027
SIATEC-CCompress	polyphonic	1289.0	24.6	5.4	0.093	0.194	0.122	0.077	0.171	0.102	0.170	0.170	0.170	0.296	0.206	0.226

Table 1: Mean MIREX metrics on JKU-PDD (highest metric values in bold)

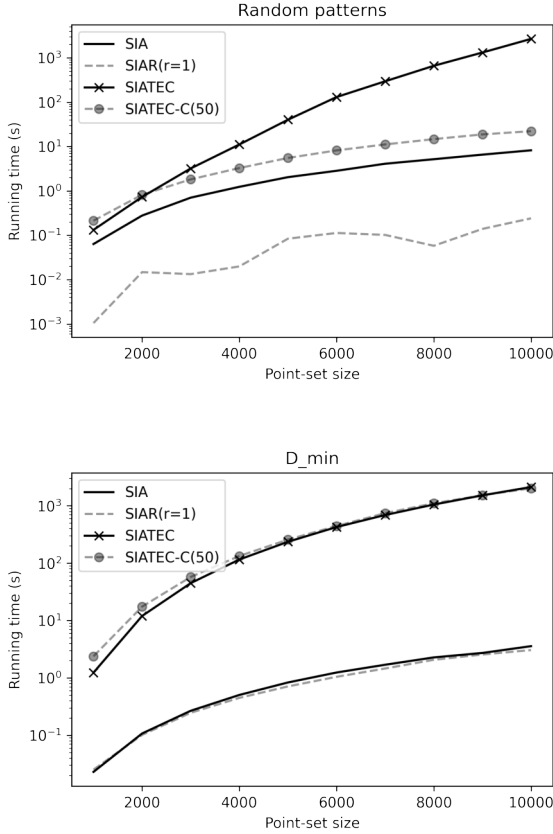


Figure 2: Running times

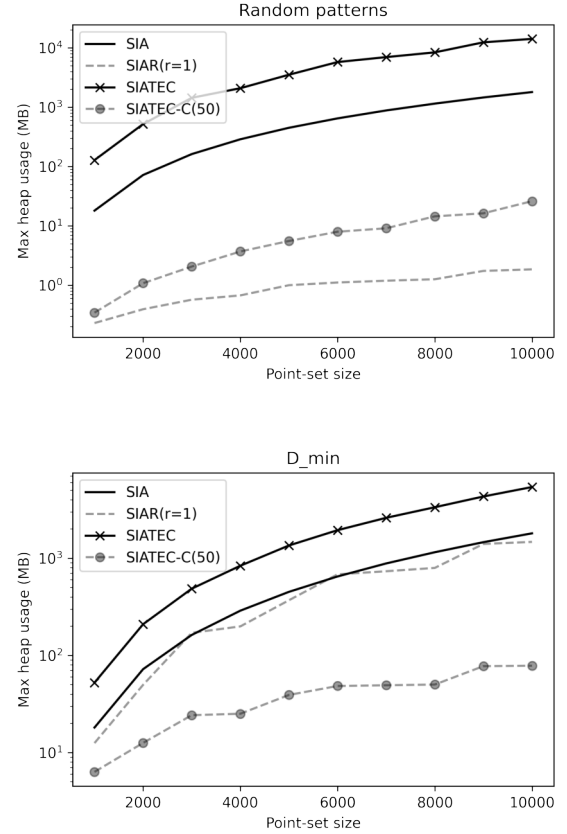


Figure 3: Maximum heap usages

music. The algorithm is based on previous research on repeated pattern discovery in polyphonic music using point-set representations of music [11].

The SIATEC-C algorithm can provide significant running time improvements over SIATEC in discovering patterns and their occurrences when the input consists of patterns that vary in size. In terms of worst-case performance, SIATEC-C does not provide improvements over SIATEC in running time. The most significant improvement SIATEC-C can provide in terms of computational efficiency is its small memory footprint, in which SIATEC-C can outperform SIAR. By keeping the memory usage small, repeated pattern discovery based on point-set representations can be applied to much longer pieces of music than previously.

The simple heuristic of cutting patterns at large IOI gaps

in SIATEC-C was found to perform at least as well as the MTP-TEC computation performed by SIATEC in terms of precision and recall. Using SIATEC-C as the TEC algorithm for the compression algorithms COSIATEC and SIATECCompress did not improve their precision or recall. A different approach to filtering and refining the patterns produced by SIATEC-C is thus needed.

The version of SIATEC-C presented in this paper uses the size of patterns as a means of prefiltering. The cover array approach can also be used with other measures that can be computed for a point-set pattern, such as compactness [11, 22]. Evaluating the musical importance of a pattern is a challenging problem. As SIATEC-C also finds all occurrences of the patterns it discovers, the algorithm can be extended with various pattern filtering methods.

## 7. ACKNOWLEDGEMENTS

This paper has benefited from discussions with Kjell Lemström and Antti Laaksonen, and from email correspondence with Tom Collins. We also thank the anonymous reviewers for their insightful comments on the paper. This work was supported by the Eemil Aaltonen Foundation grant (grant number 220014K).

## 8. REFERENCES

- [1] B. Janssen, W. B. de Haas, A. Volk, and P. van Kranenburg, "Finding repeated patterns in music: State of knowledge, challenges, perspectives," in *Sound, Music, and Motion. CMMR 2013. Lecture Notes in Computer Science*, vol. 8905, M. Aramaki, O. Derrien, R. Kronland-Martinet, and S. Ystad, Eds. Springer, Cham, 2013, pp. 277–297.
- [2] I. D. Bent and A. Pople, "Analysis," in *Grove Music Online*. Oxford University Press, 2001, accessed: 5 May 2022. [Online]. Available: <https://www.oxfordmusiconline.com/grovemusic/view/10.1093/gmo/9781561592630.001.0001/omo-9781561592630-e-0000041862>
- [3] O. Lartillot and P. Toivainen, "Motivic matching strategies for automated pattern extraction," *Musicae Scientiae, Discussion Forum 4A*, pp. 281–314, 2007.
- [4] O. Lartillot, "Automated motivic analysis: An exhaustive approach based on closed and cyclic pattern mining in multidimensional parametric spaces," in *Computational Music Analysis*, D. Meredith, Ed. Springer International Publishing, 2016, pp. 273–302.
- [5] D. Meredith, "Using point-set compression to classify folk songs," in *The Fourth International Workshop on Folk Music Analysis (FMA 2014)*, Istanbul, Turkey, 2014.
- [6] P. Allegraud, L. Bigo, L. Feisthauser, M. Giraud, R. Grould, E. Leguy, and F. Levé, "Learning sonata form structure on mozart's string quartets," *Transactions of the International Society for Music Information Retrieval*, vol. 2, no. 1, pp. 82–96, 2019.
- [7] T. Collins, A. Arzt, H. Frostel, and G. Widmer, "Using geometric symbolic fingerprinting to discover distinctive patterns in polyphonic music corpora," in *Computational Music Analysis*, D. Meredith, Ed. Springer International Publishing, 2016, pp. 445–474.
- [8] C. Louboutin and D. Meredith, "Using general-purpose compression algorithms for music analysis," *Journal of New Music Research*, vol. 45, no. 1, pp. 1–16, 2016.
- [9] D. Meredith, "Analysis by compression: Automatic generation of compact geometric encodings of musical objects," in *The Music Encoding Conference*, Mainz, Germany, 2013.
- [10] D. Conklin, "Mining contour sequences for significant closed patterns," *Journal of Mathematics and Music*, vol. 15, no. 2, pp. 112–124, 2021. [Online]. Available: <https://doi.org/10.1080/17459737.2021.1903591>
- [11] D. Meredith, K. Lemström, and G. A. Wiggins, "Algorithms for discovering repeated patterns in multidimensional representations of polyphonic music," *Journal of New Music Research*, vol. 31, no. 4, pp. 321–345, 2002.
- [12] K. Lemström, *String Matching Techniques for Music Retrieval*. PhD thesis, University of Helsinki, 2000.
- [13] D. Conklin and C. Anagnostopoulou, "Representation and discovery of multiple viewpoint patterns," in *Proceedings of the International Computer Music Conference (ICMC 2001)*, La Habana, Cuba, 2001.
- [14] G. Velarde, D. Meredith, and T. Weyde, "A wavelet-based approach to pattern discovery in melodies," in *Computational Music Analysis*, D. Meredith, Ed. Springer International Publishing, 2016, pp. 303–333.
- [15] D. Humphreys, K. Sidorov, A. Jones, and D. Marshall, "An investigation of music analysis by the application of grammar-based compressors," *Journal of New Music Research*, vol. 50, no. 4, pp. 312–341, 2021. [Online]. Available: <https://doi.org/10.1080/09298215.2021.1978505>
- [16] E. Ukkonen, K. Lemström, and V. Mäkinen, "Geometric algorithms for transposition invariant content-based music retrieval," in *Proceedings of the 4th International Conference on Music Information Retrieval (ISMIR 2003)*, Baltimore, Maryland, USA, 2003.
- [17] D. Meredith, "Analysing music with point-set compression algorithms," in *Computational Music Analysis*, D. Meredith, Ed. Springer International Publishing, 2016, pp. 335–366.
- [18] A. Laaksonen and K. Lemström, "On the memory usage of the SIA algorithm family for symbolic music pattern discovery," in *Eighth International Conference on Mathematics and Computation in Music*, 2022, in press.
- [19] T. Collins, *Improved methods for pattern discovery in music, with applications in automated stylistic composition*. PhD thesis, The Open University, 2011.
- [20] A. Laaksonen and K. Lemström, "Transposition and time-warp invariant algorithm for detecting repeated patterns in polyphonic music," in *6th International Conference on Digital Libraries for Musicology*, 2019.
- [21] A. Laaksonen, K. Lemström, and O. Björklund, "Transposition and time-scaling invariant algorithm for detecting repeated patterns in polyphonic music," in *Eighth International Conference on Mathematics and Computation in Music*, 2022, in press.

- [22] D. Meredith, “COSIATEC and SIATECCompress: Pattern discovery by geometric compression,” in *MIREX 2013. Competition on Discovery of Repeated Themes and Sections*, Curitiba, Brazil, 2013.
- [23] J. C. Forth, *Cognitively-motivated geometric methods of pattern discovery and models of similarity in music*. PhD thesis, Department of Computing, Goldsmiths, University of London, 2012.
- [24] D. Meredith, “RecurSIA-RRT: Recursive translatable point-set pattern discovery with removal of redundant translators,” in *Machine Learning and Knowledge Discovery in Databases*, P. Cellier and K. Driessens, Eds. Cham: Springer International Publishing, 2019, pp. 485–493.
- [25] T. Collins and D. Meredith, “Maximal translational equivalence classes of musical patterns in point-set representations,” in *Mathematics and Computation in Music: 4th International Conference, MCM 2013, Proceedings. Lecture Notes in Computer Science, Vol. 7937*. Springer, Berlin, 2013, pp. 88–99.
- [26] T. Collins, J. Thurlow, R. Laney, A. Willis, and P. H. Garthwaite, “A comparative evaluation of algorithms for discovering translational patterns in baroque keyboard works,” in *Proceedings of the 11th International Society for Music Information Retrieval Conference (ISMIR 2010)*, Utrecht, Netherlands, 2010.
- [27] A. Arzt, S. Böck, and G. Widmer, “Fast identification of piece and score position via symbolic fingerprinting,” in *Proceedings of the 13th International Conference on Music Information Retrieval (ISMIR 2012)*, Porto, Portugal, 2012.
- [28] T. Collins, A. Arzt, S. Flossmann, and G. Widmer, “SIARCT-CFP: Improving precision and the discovery of inexact musical patterns in point-set representations,” in *Proceedings of the 14th International Society for Music Information Retrieval Conference (ISMIR 2013)*, Curitiba, Brazil, 2013.
- [29] G. A. Wiggins, “Models of musical similarity,” in *Musicae Scientiae, Discussion Forum 4A*, 2007, pp. 315–338.
- [30] O. Björklund, *Improving the running time of repeated pattern discovery in multidimensional representations of music*. Master’s Thesis, University of Helsinki, 2018. [Online]. Available: <https://ethesis.helsinki.fi/repository/handle/123456789/21114>
- [31] T. Collins, “Mirex 2013 competition: Discovery of repeated themes and sections,” 2013, accessed: 12 April 2022. [Online]. Available: [https://www.music-ir.org/mirex/wiki/2013:Discovery\\_of\\_Repeated\\_Themes\\_%26\\_Sections](https://www.music-ir.org/mirex/wiki/2013:Discovery_of_Repeated_Themes_%26_Sections)

# TAILED U-NET: MULTI-SCALE MUSIC REPRESENTATION LEARNING

Marcel A. Vélez Vásquez

Music Cognition Group · Institute for Logic, Language, and Computation · University of Amsterdam  
marcel.velezv@gmail.com

John Ashley Burgoyne

j.a.burgoyne@uva.nl

## ABSTRACT

Self-supervised learning has steadily been gaining traction in recent years. In music information retrieval (MIR), one promising recent application of self-supervised learning is the CLMR framework (contrastive learning of musical representations). CLMR has shown good performance, achieving results on par with state-of-the-art end-to-end classification models, but it is strictly an encoding framework. It suffers the characteristic limitation of any encoder that it cannot explicitly combine multi-timescale information, whereas a characteristic feature of human audio perception is that we tend to perceive all frequencies simultaneously. To this end, we propose a generalization of CLMR that learns to extract and explicitly combine representations across different frequency resolutions, which we coin the tailed U-Net (TUNe). TUNe architectures combine multi-timescale information during a decoding phase, similar to U-Net architectures used in computer vision and source separation, but have a tail added to reduce sample-level information to a smaller pre-defined number of representation dimensions. The size of the decoding phase is a hyperparameter, and in the case of a zero-layer decoding phase, TUNe reduces to CLMR. The best TUNe architectures, however, require less training time to match CLMR performance, have superior transfer learning performance, and are competitive with state-of-the-art models even at dramatically reduced dimensionalities.

## 1. INTRODUCTION

Representation learning is a fast-moving sub-field of machine learning that seeks to distill information encoded in different types of input signals into less noisy abstract representations that are suitable for various downstream tasks. Such representations, which are learned without explicit supervision, have been successfully applied to a broad variety of musical and non-musical task domains [1], including audio tagging [2, 3] and speech recognition [4]. After self-supervised training, the learned representations are then evaluated by *probing*, a term originating from natural language processing [5–7]. In MIR, probing is also known as shallow network training or transfer learning [2, 8–13].

When probed, these self-supervised learning methods perform comparably to end-to-end trained models [3, 14, 15].

One of the more common learning architectures used for MIR tasks is the convolutional neural network (CNN) [16–19]. CNNs typically consist of either only an encoder path or an encoder and decoder path. One distinctive CNN with both an encoder *and* a decoder path model is the U-Net, consisting of variants of the encoder and decoder paths called contractive and expansive paths. Our work focuses specifically on adapting the U-Net architecture [20] to representation learning. To the best of our knowledge, there is little to no published research in computer vision, MIR, or signal processing that has considered the potential of U-Nets for representation learning.

U-Nets originated from the field of biomedical image segmentation, where they were introduced with the goal of being more data-efficient and less time-consuming to train for segmentation tasks, while also being able to perform well with relatively few data points and in the presence of class imbalance [20, 21]. U-Net architectures have shown top performance in segmentation, winning the ISBI cell tracking contest by a large margin in 2015 [20]. One of the arguments for how well U-Net architectures perform is the way the contractive and expansive paths allow the network to incorporate features across multiple resolutions.

U-Nets have also been shown to perform well within the audio domain. Their application to source separation in the time-frequency domain yielded state-of-the-art results [22], after which the U-Net established itself for source separation in the raw audio domain as well [23]. In raw audio and speech generation, U-Nets perform on par with Wavenet [24], with fewer parameters and faster inference [25]. We are also motivated to explore U-Net-like architectures for representation learning because of their intuitive relation to the *slow feature hypothesis* [26], which states that much of the meaningful information contained in signals changes gradually, over larger timescales. Without requiring a formal transformation to the frequency domain, U-Net architectures can extract these slow features alongside fine-grained high-frequency information by encoding and combining features across multiple timescales [25].

Given the scarcity of publicly available labelled data in MIR, we focus further on U-Nets for *self-supervised* learning. Specifically, we adapt the contrastive semi-supervised learning method from CLMR [3], since this has shown great promise on label training efficiency and generalisability of learned representations to out-of-domain MIR datasets. Specifically, we generalise the SampleCNN [27] en-



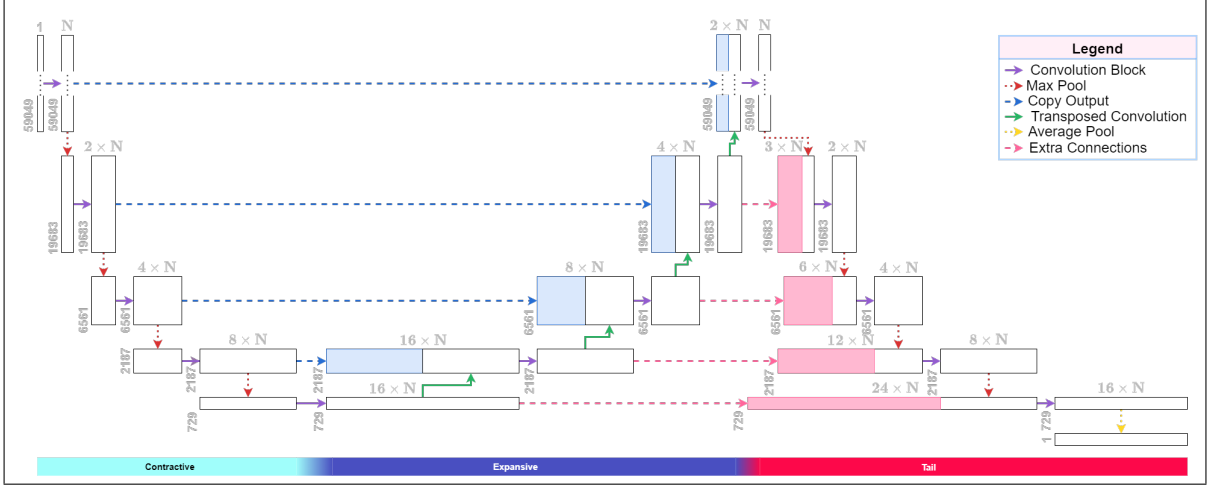


**Figure 1:** The TUNe architecture extracts features containing information obtained at multiple timescales. To this end, it consists of three main components: (1) the *contractive path* iteratively extracts features at a given timescales and reduces the signal resolution; (2) the *expansive path* upsamples the extracted features at lower resolutions and concatenates them into higher-resolution features than those obtained from the contractive path; and finally, (3) the *tail* combines the features extracted at multiple timescales and reduces their spatial resolution, ultimately yielding a single, low-dimensional, multi-timescale representation for an input signal.

coder architecture used in CLMR with a new architecture we dub the *tailed U-Net* (TUNe). TUNe architectures are like U-Net architectures, but with an additional contractive path – the tail – extending the original architecture by a mapping from a representation at the input resolution to a reduced latent representation size (see Figure 1). Intuitively, the ‘U’ shape of the network extracts a representation at the original temporal resolution, encoding a combination of slow feature patterns with higher-frequency components from the input signal, whereas the tail learns temporally reduced patterns from this enriched signal.

Our main contribution is this novel angle for the use of U-Nets for representation learning on signal data. Furthermore, we investigate a number of architectural setups with different model sizes to assess the performance and parameter efficiency of TUNe networks. In order to evaluate the learned representations, we transfer them to a range of benchmark MIR tasks, showing competitive performance with a drastically shortened training regime, parameter count, and representation dimensionality.

## 2. RELATED WORK

State-of-the art algorithms for audio-based MIR tasks (e.g., chord recognition, key detection, and music audio tagging) are generally built on one of three input forms: (1) time-frequency representations of the audio signal, (2) raw time-domain audio, or (3) a combination of raw audio and time-frequency representations [28]. Among the top-performing raw audio input architectures are musicCNN [2], JukeBox [29], and SampleCNN [27]. SampleCNN was introduced for raw audio classification and later adapted for CLMR’s contrastive learning setting. We use CLMR’s version of SampleCNN as a reference point for both performance and number of parameters. Moreover,

the TUNe convolution blocks introduced in Section 3 are based on the filter–stride–max pooling operation used in SampleCNN, which downshifts the effective frequency range modelled by the convolution kernels applied in subsequent layers. Note that because of this use of pooling operations, much high-frequency information is discarded in the extraction of the encoding from the input. Instead, our proposed approach explicitly combines these subsampled lower-frequency features with high-frequency features obtained at the original temporal resolution.

For a range of benchmark MIR datasets, CLMR is currently the best-performing self-supervised model that does not require industry-scale hardware to train [14]. It is a self-supervised learning framework, and as such, it requires no labelled data for training. Specifically, it is a contrastive learning framework: given two similar inputs to the network (e.g., two segments from the same song), the loss function is designed to ensure that the learned representations of these samples should lie closer to each other than the representations of samples from two different songs. CLMR also includes music-specific data augmentations to ensure a robust representation learning framework for MIR, for example, transposing the pitch of a segments up or down and still instructing the network to predict a closer distance to the original fragment than to the other audio segments in the batch. Because mapping the representations with a projector head instead of directly using the network representation results in a better representations [30], the output layer is replaced with an identity function and a projector head is added to the models trained with CLMR.

## 3. TAILED U-NET ARCHITECTURES

The architecture for representation learning we explore in this work is based on the traditional U-Net [20]. The U-